Polymer 50 (2009) 2578–2586

Contents lists available at ScienceDirect

Polymer

journal homepage: www.elsevier.com/locate/polymer

Synthesis of pH-sensitive hollow polymer microspheres with movable magnetic core

Guangyu Liu, Hui Wang, Xinlin Yang*

Key Laboratory of Functional Polymer Materials, The Ministry of Education, Institute of Polymer Chemistry, Nankai University, Tianjin 300071, China

ARTICLE INFO

Article history:
Received 18 November 2008
Received in revised form
25 March 2009
Accepted 3 April 2009
Available online 12 April 2009

Keywords:
pH-sensitive
Hollow polymer microspheres
Distillation precipitation polymerization

ABSTRACT

The pH-sensitive hollow poly(*N*,*N*′-methylenebisacrylamide-*co*-methacrylic acid) (P(MBAAm-*co*-MAA)) microspheres with movable magnetic/silica (Fe_3O_4/SiO_2) cores were prepared by the selective removal of poly(methacrylic acid) (PMAA) layer in ethanol/water from the corresponding Fe_3O_4/SiO_2/PMAA/P(MBAAm-*co*-MAA) tetra-layer microspheres, which were synthesized by the distillation precipitation copolymerization of *N*,*N*′-methylenebisacrylamide (MBAAm) and methacrylic acid (MAA) in the presence of Fe_3O_4/SiO_2/PMAA tri-layer microspheres as seeds in acetonitrile with 2,2′-azobisisobutyronitrile (AIBN) as the initiator. The Fe_3O_4/SiO_2/PMAA tri-layer microspheres were afforded by the distillation precipitation polymerization of MAA with 3-(methacryloxy)propyl trimethoxysilane (MPS)-modified Fe_3O_4/SiO_2 core–shell particles as the seeds. The functional multi-layer inorganic/polymer microspheres and the corresponding hollow polymer microspheres with movable magnetic cores were characterized with transmission electron microscopy (TEM), Fourier-transform infrared (FT-IR) spectra, dynamic light scattering (DLS), and vibrating sample magnetometer (VSM).

1. Introduction

The development of materials with novel structure has been a fundamental focus of the chemical research, which promotes the advancement in both academic and industry fields. In these years, hollow microspheres have attracted increasing attention due to their unique properties, such as low density, high specific area, good flow ability and surface permeability, which have found applications in many fields, including catalysis, controlled-drug delivery system, artificial cells, fillers, pigments, light weight structural materials, nano-reactors, low dielectric constant materials, acoustic insulations, and photonic crystals [1–4]. A variety of physical and chemical methods have been used for the synthesis of the hollow polymer microspheres, such as the encapsulation of a hydrocarbon non-solvent [5], layer-by-layer (LbL) assembly of polymer electrolyte [6], micelle formation of block copolymers [7] and surface-initiated atom transfer radical polymerization (ATRP) [8]. Hollow particles with complex structures and unique morphology have been prepared [9–12]. An important concern of hollow microspheres is to accommodate guest nanoparticles in their cavity, which results in an interesting structure as hollow microspheres with movable cores and novel properties different from those of host hollow microspheres and the guest nanoparticles. Nanoparticles, including gold [11,13,14], silver [15], tin [16], silica [12], polymer [17], and iron oxide [18], have been incorporated into the interior of the hollow microspheres via different techniques.

Magnetic particles, for example, magnetite (Fe_3O_4) nanoparticles have various applications, such as magnetic storage media, printing inks, magnetic resonance imaging, drug delivery, biomedicine, biosensors, magnetic separation, ferro-fluid, and catalysis [19–23] due to their extraordinary magnetic, optical, and biocompatible properties. However, these nano-sized magnetite particles tend to aggregate because of their high specific area and strong interparticle interaction, which limits their utilization. Therefore, it is essential to develop strategies for the chemical stabilization of the naked magnetic nanoparticles against aggregation over a long period. The formation of magnetite/polymer hybrid/composite materials not only stabilized the magnetic nanoparticles, but also endowed the magnetic nanoparticles with functionality. In such a way, magnetic/polymer microspheres have been found wide applications in the fields of biology, medicine, catalysis and many other areas [24–28]. The preparation of magnetite/polymer particles can be generally classified as three categories. One method was to assemble magnetic particles and polymer microspheres after they were synthesized separately [29,30], which afforded composite particles with magnetic properties via physical or physicochemical interaction between these two components. The second technique was *in-situ* precipitation of iron-oxides in the

* Corresponding author. Tel.: +86 22 23502023; fax: +86 22 23503510.
E-mail address: xlyang88@nankai.edu.cn (X. Yang).

0032-3861/$ – see front matter © 2009 Elsevier Ltd. All rights reserved.
doi:10.1016/j.polymer.2009.04.002

presence of polymer microspheres, such as *in-situ* precipitation of iron-oxides within the pores of preformed porous polystyrene (PSt) seeds [31]. The third way was to *in-situ* polymerize monomers in the presence of magnetic particles, including suspension polymerization [32], emulsion polymerization [33–43], dispersion polymerization [44,45], precipitation polymerization [46], and ATRP [47]. However, it was difficult to control the distribution of the magnetite nanoparticles in the magnetic/polymer composites for emulsion polymerization [25] and the morphology of the resultant composite particles via a sol–gel process [48].

Many efforts have been paid on the preparation of smart microcontainers, in which the structure can be switched reversibly from closed state to an open state under different pH values [49], ionic strengths [50], and temperatures [51]. The "intelligent" hollow spheres with stimuli-responsive behavior may be essential for some potential applications, *e.g.* in drug delivery, which endows an effective loading of resultant capsules or releasing the encapsulated materials in a controlled way at the desired target. In this context, the preparation of pH-responsive hollow polymer microspheres with movable magnetic cores is particularly attractive, which is to fabricate the hollow spheres having characteristics controlled by the pH and the magnetic field.

In our previous work, distillation precipitation polymerization has been successfully developed as a facile technique for the synthesis of tri-layer polymer microspheres [17] and inorganic/polymer composite/hybrid microspheres [14] for the further development of the hollow polymer microspheres with movable inner core. Here, we describe the preparation of pH-sensitive polymer hollow microspheres with movable magnetic cores via the selective removal of non-crosslinked poly(methacrylic acid) (PMAA) mid-layer from the magnetite/silica/poly(methacrylic acid)/poly(*N*,*N*′-methylenebisacrylamide-*co*-methacrylic acid) (Fe_3O_4/SiO_2/PMAA/P(MBAAm-*co*-MAA)) tetra-layer microspheres, which was synthesized by the distillation precipitation polymerization of MBAAm and MAA in acetonitrile with AIBN as initiator in the presence of Fe_3O_4/SiO_2/PMAA tri-layer particles as the seeds.

2. Experimental

2.1. Chemicals

Ferric chloride ($FeCl_3 \cdot 6H_2O$) and ferrous chloride ($FeCl_2 \cdot 4H_2O$) were purchased from Tianjin Guangfu Chemical Engineering Institute and Shanghai Gongxuetuan Reagents II Co., respectively. Ammonia (25%, aqueous solution) was provided by Tianjin Dongzheng Fine Chemical Reagent Factory, China. Trisodium citrate was obtained from Tianjin Chemical Reagents I Co. Tetraethylorthosilicate ($Si(OEt)_4$, TEOS) was bought from Aldrich and used without further purification. 3-(Methacryloxy)propyl trimethoxysilane (MPS) was got from Aldrich and distilled under vacuum. *N*,*N*′-Methylenebisacrylamide (MBAAm, chemical grade, Tianjin Bodi Chemical Engineering Co.) was recrystallized from acetone. Methacrylic acid (MAA) was purchased from Tianjin Chemical Reagent II Co. 2,2′-Azobisisobutyronitrile (AIBN) was provided by Chemical Factory of Nankai University and recrystallized from methanol. Acetonitrile (analytical grade, Tianjin Chemical Reagents II Co.) was dried over calcium hydride and purified by distillation before use. All the other reagents were of analytical grade and used without any further treatment.

2.2. Synthesis of MPS-modified magnetite/silica nanoparticles

Fe_3O_4 nanoparticles were prepared by chemical co-precipitation of Fe^{3+} and Fe^{2+} under a basic condition. $FeCl_3 \cdot 6H_2O$ (27.1 g, 0.10 mol) and $FeCl_2 \cdot 4H_2O$ (9.95 g, 0.05 mol) were dissolved in 50 mL of deionized water with a mechanical stirring at 60 °C, then 80 mL of ammonia was added. The dispersion was stirred for 30 min upon addition of trisodium citrate (50 g). The resultant magnetite nanoparticles were washed with deionized water with the aid of a magnet. Deionized water was then added to disperse the resultant Fe_3O_4 nanoparticles. The solid content of the magnetic fluid was 24.3 mg/mL for further synthesis.

Magnetite/silica (Fe_3O_4/SiO_2) core–shell particles were prepared according to the method in the literature [52]. 4.0 Mililiters of TEOS was slowly added to the magnetic fluid (3.5 mL) in ethanol (16.0 mL), deionized water (40.0 mL) with mechanical stirring in presence of 5 mL of 25 wt% ammonium hydroxide as catalyst. After the reaction system was stirred for 12 h, silica layer was formed on the surface of Fe_3O_4 nanoparticles.

Modification of Fe_3O_4/SiO_2 nanoparticles with MPS was achieved by introducing MPS (1.0 g, 4.0 mmol) into the above ethanol suspension of Fe_3O_4/SiO_2 nanoparticles under stirring and the mixture was stirred for 48 h further at room temperature. The resultant MPS-modified Fe_3O_4/SiO_2 nanoparticles were purified by centrifugation, decantation, and resuspension in ethanol for three cycles to remove the excessive MPS. The resultant MPS-modified Fe_3O_4/SiO_2 nanoparticles were dried in a vacuum oven at 50 °C till constant weight.

The synthesis of MPS-modified Fe_3O_4/SiO_2 nanoparticles was referred as the first-stage reaction in the present work.

2.3. Preparation of magnetite/silica/poly(methacrylic acid) tri-layer microspheres by the second-stage distillation precipitation polymerization

A typical procedure for the distillation precipitation polymerization to afford magnetite/silica/poly(methacrylic acid) (Fe_3O_4/SiO_2/PMAA) tri-layer microspheres: 0.1 g of MPS-modified Fe_3O_4/SiO_2 nanoparticles were suspended in 40 mL of acetonitrile as a black suspension for the seeds of the second-stage polymerization. Then MAA (0.20 mL, total as 0.5 vol% of the reaction system) and AIBN (0.004 g, 2 wt% relative to the monomer) were dissolved in the suspension. The two-necked flask attaching with a fractionating column, Liebig condenser and receiver was submerged in a heating mantle. The reaction mixture was heated from ambient temperature till the boiling state within 20 min and the reaction system was kept under refluxing state for further 20 min. Then the polymerization was carried out with distilling the solvent out of the reaction system and the reaction was ended after 20 mL of acetonitrile was distilled off the reaction mixture within 70 min. After the polymerization, the resultant Fe_3O_4/SiO_2/PMAA tri-layer microspheres were purified by repeating centrifugation, decantation, and resuspension in acetonitrile for three times. The tri-layer particles were dried in a vacuum oven at 50 °C till constant weight.

The other distillation precipitation polymerizations to prepare Fe_3O_4/SiO_2/PMAA tri-layer microspheres with different polymer shell thicknesses were much similar to that of the typical procedure by varying the mass ratio of MAA monomer to MPS-modified Fe_3O_4/SiO_2 seeds, while the amount of AIBN initiator was maintained at 2 wt% relative to the monomer. The treatment of these tri-layer microspheres was the same as that for the typical procedure.

2.4. Preparation of magnetite/silica/poly(methacrylic acid)/poly(*N*,*N*′-methylenebisacrylamide-co-methacrylic acid) tetra-layer microspheres by the third-stage distillation precipitation polymerization

A typical procedure for the distillation precipitation polymerization to afford magnetite/silica/poly(methacrylic acid)/poly(*N*,*N*′-methylenebisacrylamide-*co*-methacrylic acid) (Fe_3O_4/SiO_2/PMAA/

P(MBAAm-*co*-MAA)) tetra-layer microspheres: In a dried 50 mL of two-necked flask, 0.10 g of Fe_3O_4/SiO_2/PMAA tri-layer particles were suspended in 40 mL of acetonitrile as a black suspension to be used as the seeds for the third-stage distillation precipitation polymerization. Then MBAAm (0.04 g), MAA (0.36 mL, 0.037 g) and AIBN (0.008 g, 2 wt% relative to the comonomers) were dissolved in the suspension. The two-necked flask was submerged in a heating mantle. The reaction mixture was heated from ambient temperature till the boiling state within 20 min and the reaction system was kept under refluxing state for 10 min further. Then the polymerization was carried out with distilling the solvent out of the reaction system and the reaction was ended after 20 mL of acetonitrile was distilled off the reaction mixture within 70 min. After the polymerization, the resultant Fe_3O_4/SiO_2/PMAA/P(MBAAm-*co*-MAA) tetra-layer microspheres were purified by repeating centrifugation, decantation, and resuspension in acetone with ultrasonic irradiation for three times. The tetra-layer microspheres were then dried in a vacuum oven at 50 °C till constant weight.

The other distillation precipitation polymerizations to prepare Fe_3O_4/SiO_2/PMAA/P(MBAAm-*co*-MAA) tetra-layer microspheres with different P(MBAAm-*co*-MAA) shell thicknesses were much similar to that of the typical procedure by varying the mass ratio of comonomers to MPS-modified Fe_3O_4/SiO_2 seeds and MBAAm crosslinking degree, while the amount of AIBN initiator was maintained at 2 wt% relative to the comonomers. The treatment of these tetra-layer microspheres was the same as that for the typical procedure.

The crosslinking degree is referred as the mass ratio of MBAAm used in the comonomer feed for the polymerization in this work. The reproducibility of the polymerization was confirmed by several duplicate and triplicate experiments.

2.5. Preparation of hollow poly(*N,N′*-methylenebisacrylamide-*co*-methacrylic acid) microspheres with movable magnetic Fe_3O_4/SiO_2 cores

The resultant Fe_3O_4/SiO_2/PMAA/P(MBAAm-*co*-MAA) tetra-layer microspheres were immersed in ethanol/water (1/1) solution to selectively remove the non-crosslinked PMAA layer. The final hollow poly(*N,N′*-methylenebisacrylamide-*co*-methacrylic acid) (P(MBAAm-*co*-MAA)) microspheres with movable magnetic Fe_3O_4/SiO_2 inner cores were dried in a vacuum oven at 50 °C till constant weight.

2.6. Characterization

The size and morphology of magnetite nanoparticles, Fe_3O_4/SiO_2 core–shell nanoparticles, Fe_3O_4/SiO_2/PMAA tri-layer microspheres, Fe_3O_4/SiO_2/PMAA/P(MBAAm-*co*-MAA) tetra-layer microspheres, and P(MBAAm-*co*-MAA) microspheres with movable magnetic Fe_3O_4/SiO_2 inner cores were determined by transmission electron microscopy (TEM, Technai G2 20-S-TWIN).

Fourier-transform infrared (FT-IR) spectra were scanned over the range of 400–4000 cm^{-1} with potassium bromide slice on a Bio-Rad FTS135 FT-IR spectrometer.

The magnetic properties of Fe_3O_4/SiO_2 core–shell nanoparticles, Fe_3O_4/SiO_2/PMAA tri-layer microspheres, Fe_3O_4/SiO_2/PMAA/P(MBAAm-*co*-MAA) tetra-layer microspheres, and P(MBAAm-*co*-MAA) microspheres with movable magnetic Fe_3O_4/SiO_2 inner cores were studied with a vibrating sample magnetometer (9600 VSM, BDJ Electronics Inc., Troy MI, US) at room temperature.

Dynamic light scattering (DLS) measurements were performed in a laser scattering spectrometer (BI-200 SM) equipped with a digital correlation (BI-10000 AT) at 636 nm and the scattering angle for the DLS measurement was 90°. All the samples were prepared from the suspension with concentration of about 1 mg/mL after ultrasonic irradiation and were then measured at pH of 3.0, 7.0 and 11.0, respectively. The hydrodynamic diameter (D_h) and the polydispersity index of the size distribution were obtained by a cumulant analysis.

3. Results and discussion

Without surface modification, the magnetite nanoparticles were prone to aggregate in the solvent due to their high specific surface area. Coating of magnetite nanoparticles with a silica layer may prevent the aggregation, which also improved the chemical stability of the composite nanoparticles under rigid condition. The encapsulation of a silica layer over magnetic Fe_3O_4 nanoparticles has been successfully performed in the literature [52].

3.1. Preparation of Fe_3O_4/SiO_2/PMAA tri-layer microspheres

Scheme 1 illustrates the synthesis of Fe_3O_4/SiO_2/PMAA/P(MBAAm-*co*-MAA) tetra-layer microspheres and the further development of pH-responsive hollow P(MBAAm-*co*-MAA) microspheres with movable magnetic Fe_3O_4/SiO_2 cores.

Magnetite (Fe_3O_4) nanoparticles were prepared by the chemical co-precipitation of Fe(III)/Fe(II) (2/1 in molar ratio) salts in an NH_4OH solution at 60 °C via a well-known sol–gel process. The typical TEM micrograph of the resultant Fe_3O_4 nanoparticles with the average diameter about 10 nm is shown in Fig. 1A, in which small aggregation of several magnetite nanoparticles was observed due to the strong magnetic dipolar interaction among these particles.

Magnetite/silica (Fe_3O_4/SiO_2) nanoparticles were prepared according to the method in the literature [52]. The silica shell was encapsulated onto Fe_3O_4 nanoparticles via a modified Stöber method in ethanol/water mixture under mild basic condition at room temperature. The TEM image of Fe_3O_4/SiO_2 core-shell nanoparticle with average diameter of 214 nm is shown in Fig. 1B, in which several Fe_3O_4 nanoparticles (deep color) with good dispersion in the center and slighter contrast of silica shell-layer for each core-shell particle. In other words, the silica shell layer with a thickness around 80 nm was coated over Fe_3O_4 nanoparticles via a hydrolysis and condensation of TEOS, which permitted the further modification of the inorganic nanoparticles with MPS.

In our previous work, monodisperse silica/polydivinylbenzene (SiO_2/PDVB) and silica/poly(ethyleneglycoldimethacrylate) (SiO_2/PEGDMA) core–shell hybrid microspheres were facilely synthesized by distillation precipitation polymerization of divinylbenzene (DVB) and ethyleneglycoldimethacrylate (EGDMA) in neat acetonitrile with MPS-modified silica particles as seeds in the absence of any additive [53], in which the reactive vinyl groups on the surface of the seeds played an important role for the encapsulation of the polymer shell layer over the silica seeds via the capture of the newly formed oligomers and monomers during the polymerization. In the present work, MPS-modified magnetite/silica nanoparticles were used as the seeds for the preparation of Fe_3O_4/SiO_2/PMAA tri-layer microspheres as shown in Scheme 1.

The surface modification of the magnetite/silica nanoparticles by the hydrolysis of MPS with the aid of surface hydroxyl groups on the surface of Fe_3O_4/SiO_2 particles was confirmed by FT-IR spectrum as shown in Fig. 2a, which displayed bands at 1634 and 1703 cm^{-1} corresponding to the stretching vibration of the vinyl groups and carbonyl units of MPS component, respectively. These reactive vinyl groups permitted the growth of the Fe_3O_4/SiO_2 nanoparticles by radical capture of the newly formed PMAA oligomers and MAA monomers during the second-stage distillation precipitation polymerization to afford Fe_3O_4/SiO_2/PMAA tri-layer microspheres as shown by TEM micrographs in Fig. 3A–C, in which

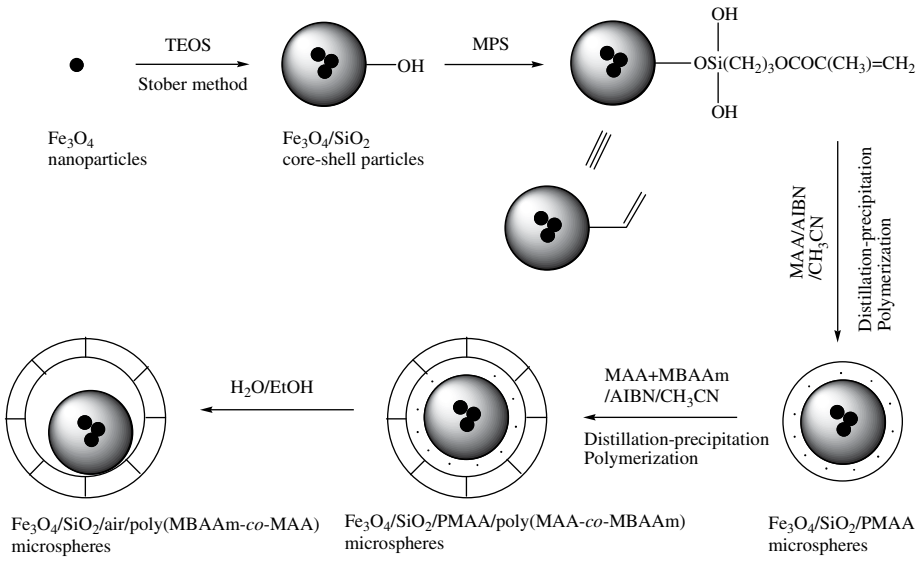

Scheme 1. Preparation of pH-sensitive hollow P(MBAAm-*co*-MAA) microspheres with movable magnetic Fe_3O_4/SiO_2 cores.

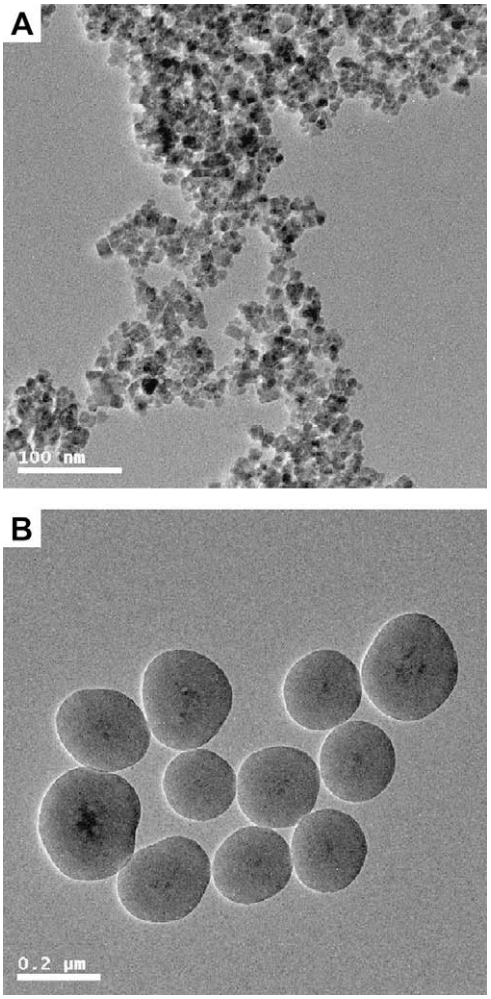

Fig. 1. TEM micrographs: A) Fe_3O_4 nanoparticles; B) MPS-modified Fe_3O_4/SiO_2 core–shell particles.

lighter contrast PMAA outer shell layer, darker silica mid-layer and the deepest small aggregates of magnetite in the center were clearly observed. The formation of monodisperse PMAA microspheres [54] indicated that acetonitrile met the solvency conditions requirement for the polymerization of MAA, during which acetonitrile dissolved the MAA monomer but precipitated the resultant PMAA species to grow the PMAA microspheres via the efficient interchain hydrogen-bonding interaction between the carboxylic acid groups. The results in Fig. 3A–C indicated that the resultant Fe_3O_4/SiO_2/PMAA tri-layer microspheres had spherical shapes with smooth and non-segmented surface without formation of any secondary-initiated particles in the cases of MAA feed ranging from 0.20 to 0.40 mL for the second-stage polymerization. This implied that the reactive surface vinyl groups on the surface of MPS-modified Fe_3O_4/SiO_2 nanoparticles captured all the newly formed PMAA oligomers and the growth of the tri-layer microspheres was performed via the efficient interchain hydrogen-bonding interaction between the carboxylic acid groups of PMAA species during the polymerization. The successful encapsulation of PMAA onto

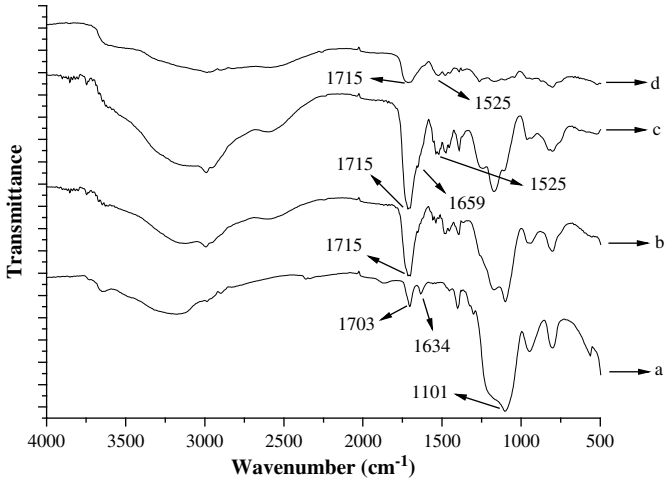

Fig. 2. FT-IR spectra of multi-layer particles: a) MPS-modified Fe_3O_4/SiO_2 core–shell particles; b) Fe_3O_4/SiO_2/PMAA tri-layer microspheres; c) Fe_3O_4/SiO_2/PMAA/P(MBAAm-*co*-MAA) tetra-layer microspheres; d) hollow P(MBAAm-*co*-MAA) microspheres with movable magnetic Fe_3O_4/SiO_2 cores.

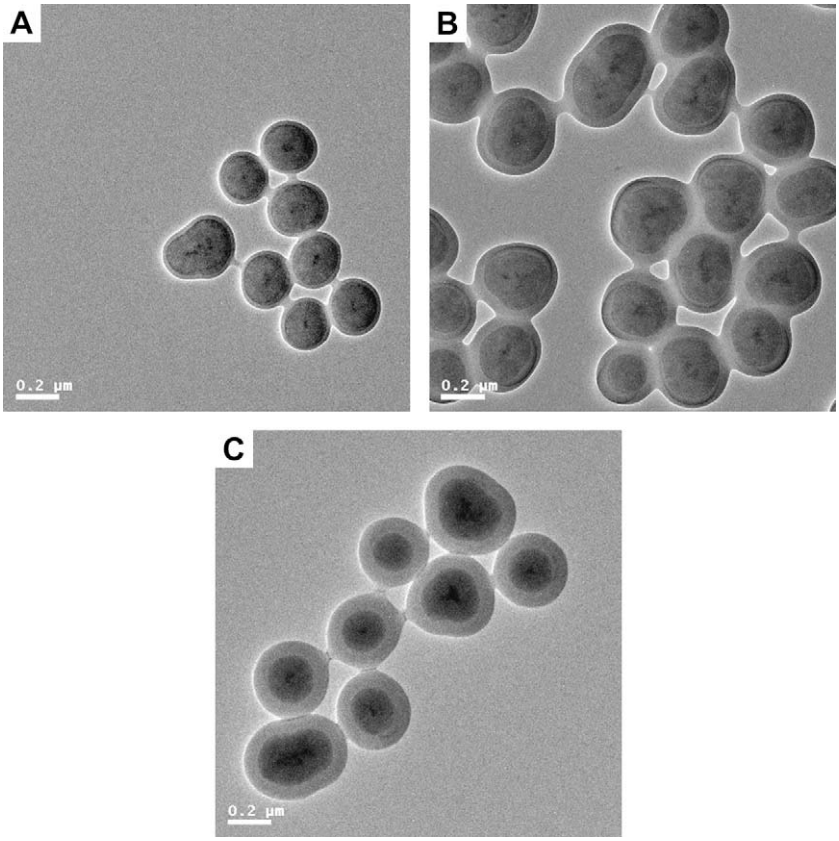

Fig. 3. TEM micrographs of Fe_3O_4/SiO_2/PMAA tri-layer microspheres with different MAA loadings: A) 0.20 mL; B) 0.30 mL; C) 0.40 mL.

MPS-modified Fe_3O_4/SiO_2 nanoparticles was proven further by the FT-IR spectrum in Fig. 2b with the presence of a strong peak at 1715 cm^{-1} assigning to the stretching vibration of the carboxylic acid groups.

The reaction conditions and diameters of the resultant Fe_3O_4/SiO_2/PMAA tri-layer microspheres PMAA tri-layer microspheres, and the conversion of MAA during the second-stage polymerization are summarized in Table 1. The size of the tri-layer microspheres was increased from 214 nm of MPS-modified Fe_3O_4/SiO_2 core–shell seeds with increasing MAA feed ranging from 0.20 to 0.40 mL and the maximum diameter with 328 nm for the resultant Fe_3O_4/SiO_2/PMAA tri-layer microspheres was obtained at MAA loading of 0.40 mL. Here, the thickness of the polymer shell layer was calculated as the half of the difference between the diameter of the resultant multi-layer microspheres and that of the corresponding seeds. In other words, Fe_3O_4/SiO_2/PMAA tri-layer microspheres with PMAA shell thicknesses ranging from 17 to 57 nm were conveniently controlled by varying the MAA monomer loading during the second-stage polymerization. The conversion of MAA to the tri-layer microspheres during the encapsulation was increased significantly from 9% to 27% when MAA loading was slightly enhanced from 0.20 to 0.40 mL. This led to the considerable increase of the size of the resultant Fe_3O_4/SiO_2/PMAA tri-layer microspheres, as there were not any secondary-initiated particles formed during the second-stage polymerization.

Table 1
The reaction conditions, size and yield of Fe_3O_4/SiO_2/PMAA tri-layer microspheres.

Entry	Magnetite/SiO_2 (g)	MAA (mL)	D_n (nm)	PMAA shell thickness (nm)	Conversion[b] (%)
A[a]	0.1	0	214	0	0
B	0.1	0.2	248	17	9
C	0.1	0.3	281	34	19
D	0.1	0.4	328	57	27

[a] MPS-modified magnetite/SiO_2 core.
[b] Conversion $= (M_{core-shell} - M_{core})/M_{MAA} \times 100\%$.

3.2. *Preparation of Fe_3O_4/SiO_2/PMAA/P(MBAAm-co-MAA) tetra-layer microspheres by the third-stage distillation precipitation polymerization*

In our previous work, poly(divinylbenzene-*co*-acrylic acid)/poly(acrylic acid)/poly(divinylbenzene-*co*-acrylic acid) tri-layer microspheres were prepared by a three-stage distillation precipitation polymerization [17], in which the hydrogen-bonding interaction between the carboxylic acid groups played a key role as the driving force for the formation of monodisperse tri-layer structure polymer microspheres. Here, Fe_3O_4/SiO_2/PMAA/P(MBAAm-*co*-MAA) tetra-layer microspheres were synthesized by the third-stage distillation precipitation copolymerization of MBAAm as crosslinker and functional MAA monomer in the presence of Fe_3O_4/SiO_2/PMAA tri-layer particles as seeds. MBAAm has been widely used as the crosslinker for the synthesis of hydrophilic microparticles, especially for stimulus-sensitive hydrogels, which can undergo large phase transition in response to small changes in the environment including pH [55], temperature [56], solvent composition [57], ion concentration [58], electrical field [59] and light [60]. The encapsulation of P(MBAAm-*co*-MAA) outer shell layer onto Fe_3O_4/SiO_2/PMAA tri-layer seeds was driven by the synergic hydrogen-bonding interaction between the carboxylic acid groups on the surface of the tri-layer particle seeds and amide group of PMBAAm component as well as the carboxylic acid groups of PMAA component in P(MBAAm-*co*-MAA) network. The typical TEM micrographs of the resultant Fe_3O_4/SiO_2/PMAA/P(MBAAm-*co*-MAA) tetra-layer microspheres are shown in Fig. 4,

which indicated that the final tetra-layer microspheres had spherical shape and smooth surface in the absence of any secondary-initiated irregular particles. These results demonstrated that the synergic hydrogen-bonding interaction during the third-stage polymerization favored the efficient capture of the radical oligomers and monomers from the solution to grow the particles further for the construction of Fe_3O_4/SiO_2/PMAA/P(MBAAm-*co*-MAA) tetra-layer microspheres. The formation of P(MBAAm-*co*-MAA) outer shell layer was confirmed by FT-IR spectrum as shown in Fig. 2c with the presence of the characteristic peaks at 1659 and 1525 cm^{-1} corresponding to the stretching vibration of the carbonyl unit and the bending vibration of *N–H* for PMBAAm component in P(MBAAm-*co*-MAA) outer shell layer.

The reaction conditions, the size from TEM observation and the yield of P(MBAAm-*co*-MAA) shell layer during the third-stage polymerization for the resultant Fe_3O_4/SiO_2/PMAA/P(MBAAm-*co*-MAA) tetra-layer microspheres are summarized in Table 2. The average diameter was significantly increased from 328 nm of Fe_3O_4/SiO_2/PMAA tri-layer seeds and the maximum size (645 nm) of Fe_3O_4/SiO_2/PMAA/P(MBAAm-*co*-MAA) tetra-layer microspheres was afforded by feed of MAA 0.54 mL with MBAAm crosslinking degree of 0.10 (Entry C). The size of Fe_3O_4/SiO_2/PMAA/P(MBAAm-*co*-MAA) tetra-layer microspheres was considerably enhanced from 397 nm with MAA feed of 0.18 mL (Entry A) to 556 nm (Entry B) with MAA feed of 0.36 mL (Entry B) and further toward 645 nm (Entry C) with MAA feed of 0.54 mL, while MBAAm crosslinking degree was maintained at 0.10 in these cases. When the MBAAm crosslinking degree was increased from 0.10 (Entry B) to 0.15 (Entry E), the diameter of tetra-layer microspheres was increased from 556 nm to 607 nm. In other words, the thickness of P(MBAAm-*co*-

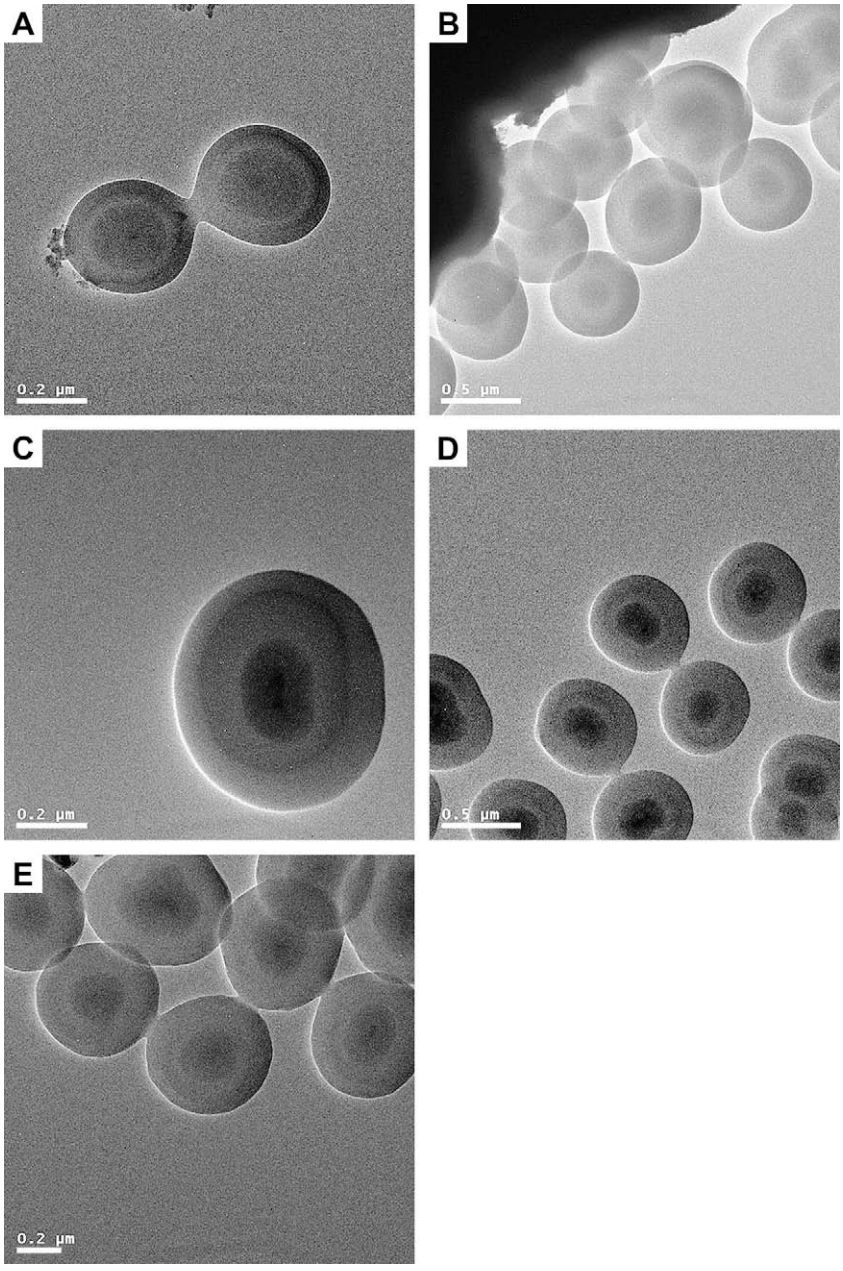

Fig. 4. TEM micrographs of Fe_3O_4/SiO_2/PMAA/P(MBAAm-*co*-MAA) tetra-layer microspheres with different MAA and MBAAm loadings: A) 0.18 mL, 0.02 g; B) 0.36 mL, 0.04 g; C) 0.54 mL, 0.06 g; D) 0.38 mL, 0.02 g; E) 0.34 mL, 0.06 g.

Table 2
The reaction conditions, size and yield of Fe_3O_4/SiO_2/PMAA/P(MBAAm-*co*-MAA) tetra-layer microspheres.

Entry	Tri-layer seeds (g)	MAA (mL)	MBAAm (g)	D_n (nm)	P(MBAAm-*co*-MAA) shell thickness (nm)	Conversion[b] (%)
A[a]	0.1	0	0	328	0	0
B	0.1	0.18	0.02	397	35	32
C	0.1	0.36	0.04	556	114	30
D	0.1	0.54	0.06	645	159	18
E	0.1	0.38	0.02	594	133	45
F	0.1	0.34	0.06	607	140	33

[a] Magnetite/SiO_2/PMAA core with PMAA shell thickness of 57 nm.
[b] Conversion $= (M_{core-shell} - M_{core})/M_{monomer} \times 100\%$.

MAA) outer shell layer can be conveniently controlled in the range of 35 and 159 nm via varying the monomer MAA feed and MBAAm crosslinking degree during the third-stage polymerization. The larger size of Fe_3O_4/SiO_2/PMAA/P(MBAAm-*co*-MAA) tetra-layer microspheres (thicker P(MBAAm-*co*-MAA) outer shell layer) was originated from the higher yields in the case of higher monomer loading and higher crosslinking degree, which was much consistent to the results in our previous work [61].

3.3. Construction of pH-sensitive P(MBAAm-co-MAA) hollow microspheres with movable magnetic Fe_3O_4/SiO_2 cores

The non-crosslinked PMAA mid-layer of the resultant Fe_3O_4/SiO_2/PMAA/P(MBAAm-*co*-MAA) tetra-layer microspheres was selectively removed by dissolution in ethanol/water (1/1) to afford hollow P(MBAAm-*co*-MAA) microspheres with movable Fe_3O_4/SiO_2 cores as illustrated in Scheme 1. The driving force for such removal was due to the solubility of the non-crosslinked PMAA in ethanol/water (1/1) as solvent. The typical TEM micrograph of hollow P(MBAAm-*co*-MAA) microspheres with movable Fe_3O_4/SiO_2 cores is shown in Fig. 5, in which the convincing hollow microspheres were clearly observed with the presence of circular rings of sectional spheres with an inner movable Fe_3O_4/SiO_2 core and an interior cavity in the mid-layer. The spherical shape was well maintained after the selective removal of the PMAA mid-layer in Fig. 5, which implied that hollow P(MBAAm-*co*-MAA) microspheres with thickness of 114 nm were enough to support the cavity during the etching process. It was believed that the magnetic Fe_3O_4/SiO_2 cores in the hollow P(MBAAm-*co*-MAA) spheres were free to move as filled with solvent, as the Fe_3O_4/SiO_2 cores were not located in the center of the hollow P(MBAAm-*co*-MAA) microspheres for TEM images in Fig. 5. However, the hollow P(MBAAm-*co*-MAA) microspheres with thickness of 35 nm (Entry A in Table 2, TEM micrograph not shown here) collapsed during the formation of the hollow structure, which implied that P(MBAAm-*co*-MAA) shell was not thick and strong enough to support the cavity formed by selective dissolution of PMAA mid-layer may be due to the low crosslinking degree in this case (0.10).

Since the sensitivity of the hollow polymer particles toward the changes in pH of environment is the basic requirement for their application as controlled drug release, the pH-responsive behavior of P(MBAAm-*co*-MAA) hollow microspheres with movable magnetic Fe_3O_4/SiO_2 cores in solutions under different pH values was investigated. The hydrodynamic diameters from DLS characterization and the corresponding polydispersity index of the resultant P(MBAAm-*co*-MAA) hollow microspheres with movable magnetic Fe_3O_4/SiO_2 cores as a function of varying pH are

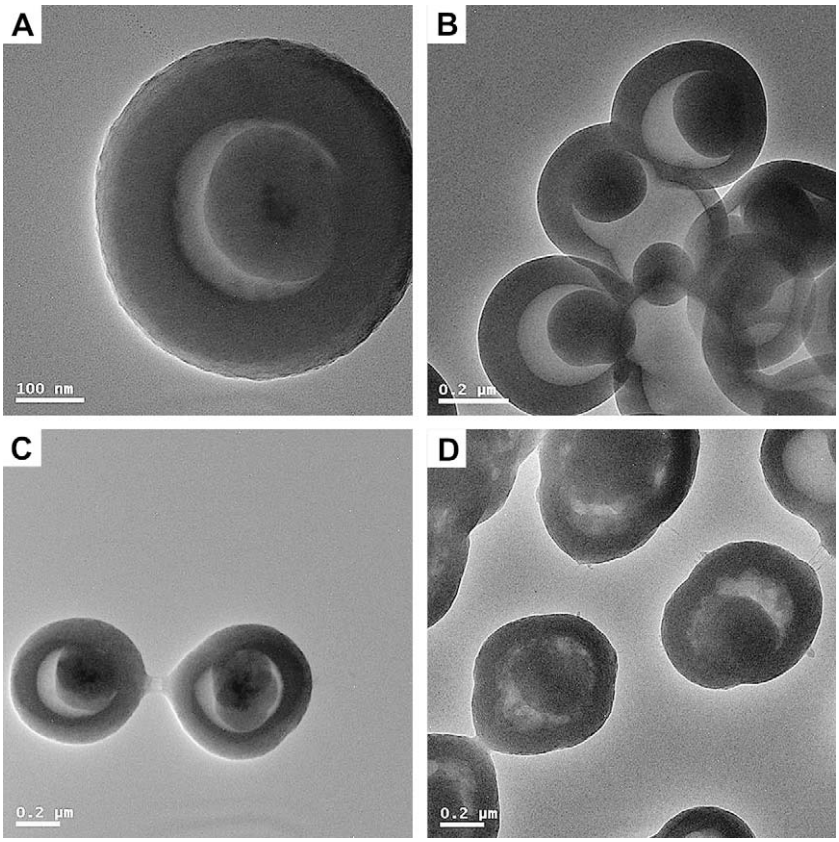

Fig. 5. TEM micrographs of hollow P(MBAAm-*co*-MAA) microspheres with movable magnetic Fe_3O_4/SiO_2 cores with different P(MBAAm-*co*-MAA) thicknesses: A) 114 nm; B) 159 nm; C) 155 nm; D) 140 nm.

Table 3
Hydrodynamic diameters of hollow P(MBAAm-*co*-MAA) microspheres with movable magnetic Fe_3O_4/SiO_2 cores at different pH values.

Magnetite/SiO_2/air/P(MBAAm-*co*-MAA)[a]	pH = 3	pH = 7	pH = 11
D_h (nm)	1153	1279	1483

[a] Magnetite/SiO_2/air/P(MBAAm-*co*-MAA) with P(MBAAm-*co*-MAA) shell thickness of 114 nm.

summarized in Table 3. The hydrodynamic size of the resultant P(MBAAm-*co*-MAA) hollow microspheres was increased significantly from 1153 nm at pH of 3 to 1279 nm at pH of 7, and further toward 1483 nm at pH of 11. These changes in diameters under different pH values were due to the partial ionization of the carboxylic acid groups of the PMAA units in P(MBAAm-*co*-MAA) shell under high pH values, resulting in Donnan osmotic swelling of the polymer network. Further, the structure of the outer P(MBAAm-*co*-MAA) shell layer can be switched reversibly from a collapsed state to a swollen state under different pH values. All the hydrodynamic diameters of P(MBAAm-*co*-MAA) microspheres (>1000 nm) were much larger than that from TEM observation (645 nm, Entry C in Table 2), which confirmed the hydrophilic property of the resultant hollow P(MBAAm-*co*-MAA) microspheres, as the former ones were obtained from a highly swollen state in aqueous solution with different pH values. Polymer microcapsules with iron oxide (γ-Fe_2O_3) magnetic nanoparticles (MPs) embedded in the polymer shell were prepared by a one-step template-free synthetic emulsion polymerization of photo-prepolymer NOS 61 with UV-cutting [62], in which the polymer microcapsules were broadly distributed and formation of a collapsed hemispherical shell after drying. These were much different from the results of the hollow P(MBAAm-*co*-MAA) microspheres with pH sensitivity, good shape of the polymer shell layer and movable magnetic cores in the present work.

The magnetic properties of the multi-layer nanoparticles containing magnetite components were studied by a vibrating sample magnetometer (VSM) at room temperature. Fig. 6 shows the magnetization curves of Fe_3O_4/SiO_2 core–shell particles, Fe_3O_4/SiO_2/PMAA tri-layer microspheres, Fe_3O_4/SiO_2/PMAA/P(MBAAm-*co*-MAA) tetra-layer microspheres, hollow P(MBAAm-*co*-MAA) microspheres with movable Fe_3O_4/SiO_2 cores. For all the samples, no magnetic hysteresis loops were observed from the field-dependent magnetization plots in Fig. 5. In other words, the

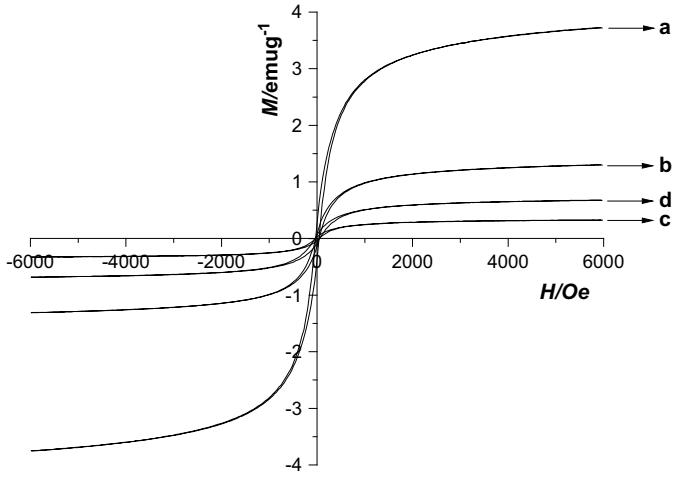

Fig. 6. Hysteresis loops for samples at room temperature: a) MPS-modified Fe_3O_4/SiO_2 core–shell particles; b) Fe_3O_4/SiO_2/PMAA tri-layer microspheres; c) Fe_3O_4/SiO_2/PMAA/P(MBAAm-*co*-MAA) tetra-layer microspheres; d) pH-sensitive hollow P(MBAAm-*co*-MAA) microspheres with movable magnetic Fe_3O_4/SiO_2 cores.

Table 4
Magnetization properties of the multi-layer structure polymer microspheres.

Entry	Saturation magnetization (emu/g)
Magnetite/SiO_2[a]	3.74
Magnetite/SiO_2/PMAA[b]	1.31
Magnetite/SiO_2/PMAA/P(MBAAm-*co*-MAA)[c]	0.33
Magnetite/SiO_2/air/P(MBAAm-*co*-MAA)[d]	0.68

[a] MPS-modified magnetite/SiO_2 core.
[b] Magnetite/SiO_2/PMAA particles with PMAA shell thickness of 57 nm.
[c] Magnetite/SiO_2/PMAA/P(MBAAm-*co*-MAA) with PMAA shell thickness of 57 nm and P(MBAAm-*co*-MAA) shell thickness of 114 nm.
[d] Magnetite/SiO_2/air/P(MBAAm-*co*-MAA) with P(MBAAm-*co*-MAA) shell thickness of 114 nm.

remanence existed when magnetic field was removed, which implied that all the magnetic particles retained paramagnetic property originating from Fe_3O_4/SiO_2 nanoparticles at room temperature. The magnetic properties of these particles are summarized in Table 4. The saturation magnetization (Ms) values for Fe_3O_4/SiO_2 core–shell particles, Fe_3O_4/SiO_2/PMAA tri-layer microspheres, Fe_3O_4/SiO_2/PMAA/P(MBAAm-*co*-MAA) tetra-layer microspheres, hollow P(MBAAm-*co*-MAA) microspheres with movable Fe_3O_4/SiO_2 cores were 3.74, 1.31, 0.33, and 0.68 emu/g as summarized in Table 4, respectively. These results indicated that the magnetization of these magnetic particles decreased considerably with the increase of polymer component due to the decrease of the effective mass of magnetite core in these cases. Furthermore, the magnetization of hollow P(MBAAm-*co*-MAA) microspheres with movable Fe_3O_4/SiO_2 cores (0.68 emu/g) was much higher than that of the corresponding Fe_3O_4/SiO_2/PMAA/P(MBAAm-*co*-MAA) tetra-layer microspheres (0.33 emu/g), which proved the efficient removal of PMAA mid-layer by simple dissolution in ethanol/water (1/1). The hollow pH-responsive P(MBAAm-*co*-MAA) microspheres with movable magnetic Fe_3O_4/SiO_2 cores can be used for controlled-release after loading of the objective drugs under high pH, especially in the case of a magnetic field. The study on the scope of this technique, including the extension to the other functional hollow structure polymer microspheres and the applications of these functional hollow microspheres, is in progress.

4. Conclusion

Hollow pH-responsive P(MBAAm-*co*-MAA) with movable magnetic Fe_3O_4/SiO_2 cores were prepared by a facile route with a three-stage reaction to afford a tetra-layer Fe_3O_4/SiO_2/PMAA/P(MBAAm-*co*-MAA) microspheres with subsequent removal of the non-crosslinked PMAA mid-layer in ethanol/water. The thicknesses of PMAA layer were conveniently controlled in the range of 17 and 57 nm by varying the MAA monomer feed during the second-stage distillation precipitation polymerization. The synergic hydrogen-bonding interaction between the carboxylic acid groups on the surface of Fe_3O_4/SiO_2/PMAA tri-layer microspheres and the amide groups of PMBAAm component as well as the carboxylic acid groups of PMAA component acted as the driving force for the formation of narrow-disperse Fe_3O_4/SiO_2/PMAA/P(MBAAm-*co*-MAA) tetra-layer microspheres during the third-stage distillation precipitation polymerization. The thickness of hollow P(MBAAm-*co*-MAA) microspheres was afforded ranging from 35 to 159 nm via changing the MAA monomer loading and MBAAm crosslinking degree for the third-stage polymerization. The hydrodynamic diameters of pH-sensitive hollow P(MBAAm-*co*-MAA) microspheres with movable magnetic Fe_3O_4/SiO_2 cores were significantly increased with higher pH in the environment, while the magnetization was increased from 0.33 emu/g of Fe_3O_4/SiO_2/PMAA/P(MBAAm-*co*-MAA) tetra-layer microspheres to 0.68 emu/g.

Acknowledgement

This work was supported by the National Natural Science Foundation of China with contract project No.: 20874049.

References

[1] Gill I, Ballesteros A. J Am Chem Soc 1998;120:8587–98.
[2] Caruso F. Adv Mater 2001;13:11–22.
[3] Cochran JK. Curr Opin Solid State Mater Sci 1998;3:474–9.
[4] Zhang J, Xu S, Kumacheva E. J Am Chem Soc 2004;126:7908–14.
[5] McDonald CJ, Bouck KJ, Chaupt AB, Stevens CJ. Macromolecules 2000;33:1593–605.
[6] Park MK, Onishi K, Looklin J, Caruso F, Advincula RC. Langmuir 2003;19:8550–4.
[7] Stewart S, Liu GJ. Chem Mater 1999;11:1048–54.
[8] Mandal TK, Fleming MS, Walt DR. Chem Mater 2000;12:3481–7.
[9] Dai ZF, Möhwald H, Tiersch B, Dähne L. Langmuir 2002;18:9533–8.
[10] Yang M, Ma J, Zhang LL, Yang ZZ, Lu YF. Angew Chem Int Ed 2005;44:6727–30.
[11] Kumata K, Lu Y, Xia YN. J Am Chem Soc 2003;125:2384–5.
[12] Zhang K, Zhang XH, Chen HT, Chen X, Zhang L, Zhang J, et al. Langmuir 2004;20:11312–4.
[13] Kim M, Sohn K, Na HB, Hyeon T. Nano Lett 2002;12:1383–7.
[14] Liu GY, Ji HF, Yang XL, Wang YM. Langmuir 2008;24:1019–25.
[15] Cheng DM, Zhou XD, Xia HB, Chao HSO. Chem Mater 2005;17:3578–81.
[16] Lee KT, Jung YS, Oh SM. J Am Chem Soc 2003;125:5652–3.
[17] Li GL, Yang XL. J Phys Chem B 2007;111:12781–6.
[18] Zhang T, Pang J, Tan G, He J, McPherson GL, Lu YF, et al. Langmuir 2007;23:5143–7.
[19] Gu H, Ho PL, Tsang KWT, Wang L, Xu B. J Am Chem Soc 2003;125:15702–3.
[20] Nam JM, Thaxton CS, Hirkin CA. Science 2003;301:1884–6.
[21] Gupta AK, Gupta M. Biomaterials 2005;26:3995–4021.
[22] Berry CC. J Mater Chem 2005;15:543–7.
[23] Lu AH, Schmidt W, Matoussevitch N, Bönnemann H, Spiethoff B, Teschen B, et al. Angew Chem Int Ed 2004;43:4303–6.
[24] Rana S, White P, Bradley M. Tetrahedron Lett 1999;40:8137–40.
[25] Liu XQ, Guan YP, Ma ZY, Liu HZ. Langmuir 2004;20:10278–82.
[26] Chen JP, Su DR. Biotechnol Prog 2001;17:369–75.
[27] Kawashita M, Tanaka M, Kokubo T, Inoue Y, Yao T, Hamada S, et al. Biomaterials 2005;26:2231–8.
[28] Deng YH, Wang CC, Shen XZ, Yang WL, Jin L, Gao H, et al. Chem Eur J 2005;11:6006–13.
[29] Xulu PM, Filipcsei G, Zrinyi M. Macromolecules 2000;33:1716–9.
[30] Jones F, Colfen H, Antonietti M. Colloid Polym Sci 2000;278:491–501.
[31] Ugelstad J, Söderberg L, Berge A, Bergström J. Nature 1983;303:95–6.
[32] Lee Y, Rho J, Jung B. J Appl Polym Sci 2003;89:2058–67.
[33] Noguchi H, Yanase N, Uchida Y, Suzuta T. J Appl Polym Sci 1993;48:1539–47.
[34] Yanase N, Noguchi H, Asakura H, Suzuta T. J Appl Polym Sci 1993;50:765–76.
[35] Xie G, Zhang QY, Luo ZP, Wu M, Li TH. J Appl Polym Sci 2003;87:1733–8.
[36] Wang PC, Chiu WY, Lee CF, Young TH. J Polym Sci Part A Polym Chem 2004;42:5695–705.
[37] Wormuth K. J Colloid Interface Sci 2001;241:366–77.
[38] Liu ZL, Ding ZH, Yao KL, Tao J, Du GH, Lu QH, et al. J Magn Magn Mater 2003;265:98–105.
[39] Dresco PA, Zaitesev VS, Gambino RJ, Chu B. Langmuir 1999;15:1945–51.
[40] Deng Y, Wang L, Yang W, Fu SK, Elaissari A. J Magn Magn Mater 2003;257:69–78.
[41] Landfester K. Adv Mater 2001;13:765–8.
[42] Csetneki I, Faix MK, Szilagyi A, Kovacs AL, Nemeth Z, Zrinyi M. J Polym Sci Part A Polym Chem 2004;42:4802–8.
[43] Xu ZZ, Wang CC, Yang WL, Deng YH, Fu SK. J Magn Magn Mater 2004;277:136–43.
[44] Horak D, Semenyuk N, Lednicky F. J Polym Sci Part A Polym Chem 2003;41:1848–63.
[45] Horak D, Benedyk N. J Polym Sci Part A Polym Chem 2004;42:5827–37.
[46] Zaitsev VS, Filimonov DS, Presnyakov IA, Gambino RJ, Chu B. J Colloid Interface Sci 1999;212:49–57.
[47] Vestal CR, Zhang ZJ. J Am Chem Soc 2002;124:14312–3.
[48] Liu QX, Xu ZH, Finch JA, Egerton R. Chem Mater 1998;10:3936–40.
[49] Sauer M, Streich D, Meier W. Adv Mater 2001;13:1649–51.
[50] Ibarz G, Dahen L, Donath E, Möhwald H. Adv Mater 2001;13:1324–7.
[51] Zha LS, Zhang Y, Yang ML, Fu SK. Adv Mater 2002;14:1090–2.
[52] Deng YH, Wang CC, Hu JH, Yang WL, Fu SK. Colloid Surf A 2005;262:87–93.
[53] Liu GY, Zhang H, Yang XL, Wang YM. Polymer 2007;48:5896–904.
[54] Bai F, Huang B, Yang XL, Huang WQ. Eur Polym J 2007;43:3923–32.
[55] Siegelm RA, Firestone BA. Macromolecules 1988;21:3254–9.
[56] Shibayama M, Mizutani S, Nomura S. Macromolecules 1996;29:2019–24.
[57] Hirokawa Y, Tanaka T, Saito E. Macromolecules 1985;18:2782–4.
[58] Park TG, Hoffman AS. Macromolecules 1993;26:5045.
[59] Tanaka T, Nishio I, Sun ST, Ueno-Nishio S. Science 1982;218:467–9.
[60] Suzuki A, Tanaka T. Nature 1990;346:345–7.
[61] Bai F, Yang XL, Huang WQ. Macromolecules 2004;37:9746–52.
[62] Koo HY, Chang ST, Choi WS, Park JH, Kim DY, Velev OD. Chem Mater 2006;18:3308–13.